

# Bulk Compton Emission of Blazar Sources

**Rafał Moderski**

*Nicolaus Copernicus Astronomical Center, Warsaw*

## Outline

1. Bulk motion in jets.
2. Bulk Comptonization close to the central black hole and accretion disk.
3. Soft X-ray “bump”.
4. Soft X-ray precursors.
5. Bulk Comptonization at larger scales.
6. Summary.

# Bulk motion in jets

NGC 6251

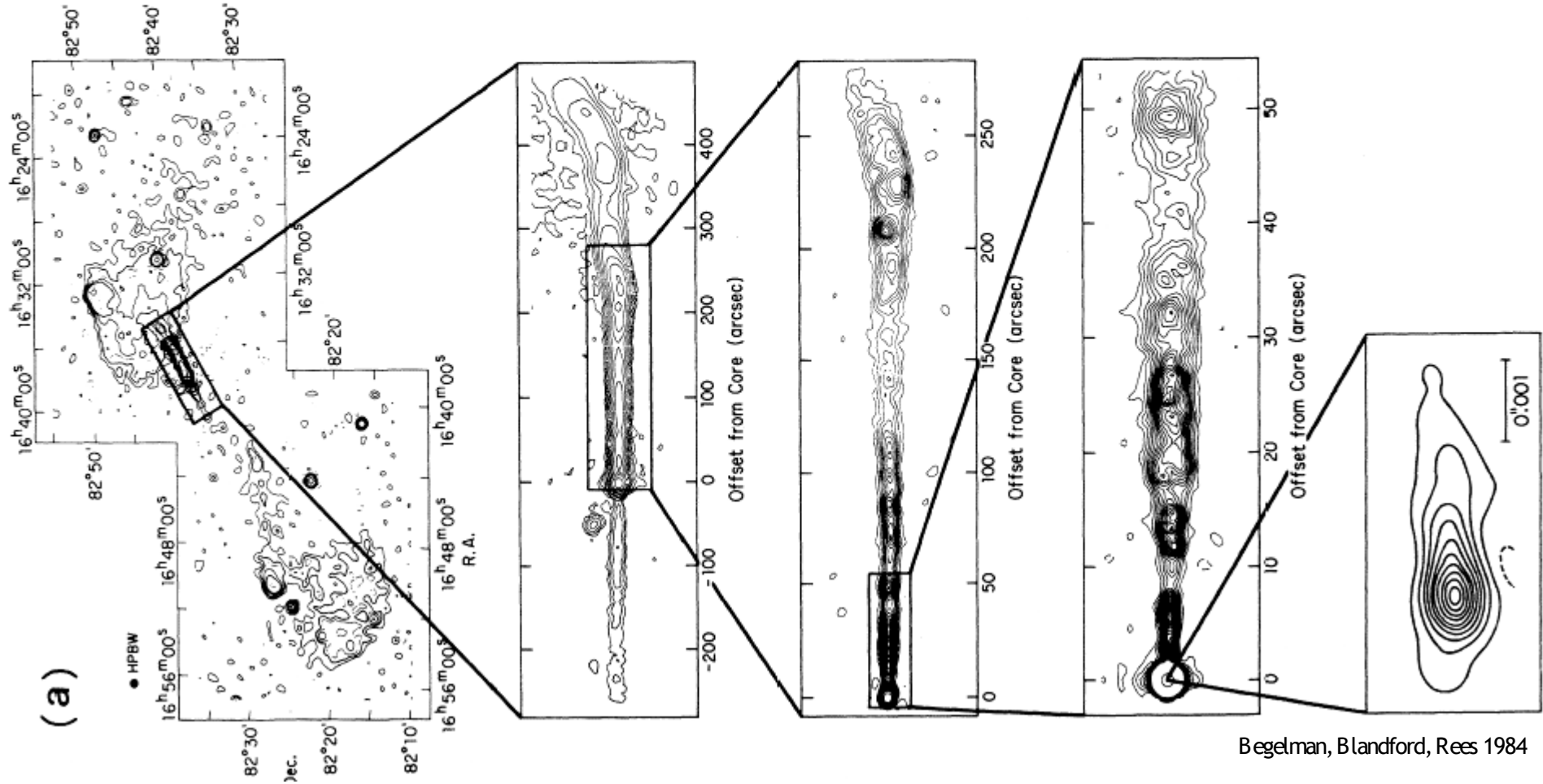
WSRT  
610 MHz

VLA  
1664 MHz

VLA  
1410 MHz

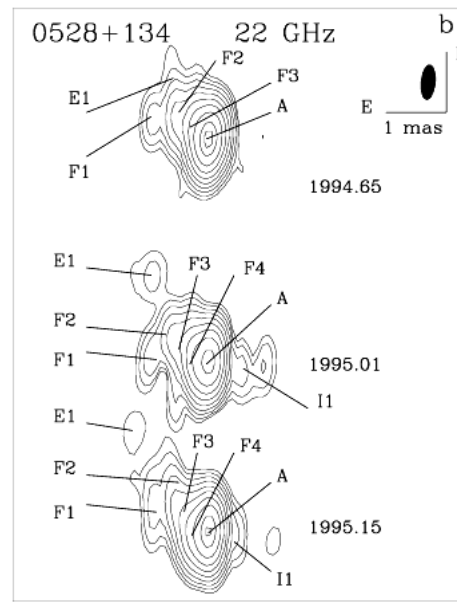
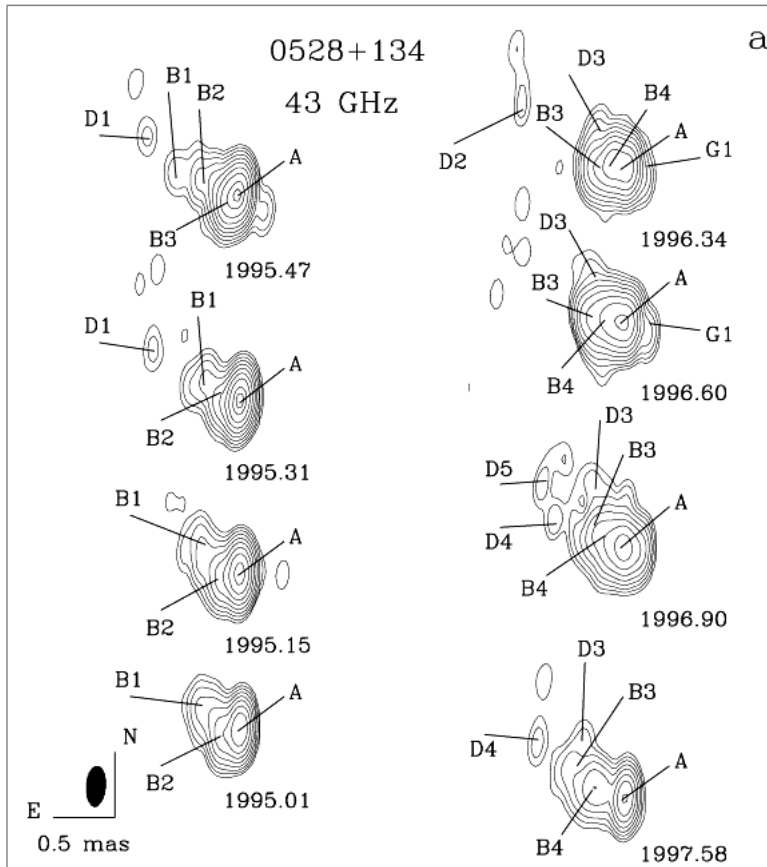
VLA  
1662 MHz

VLB  
10651 MHz

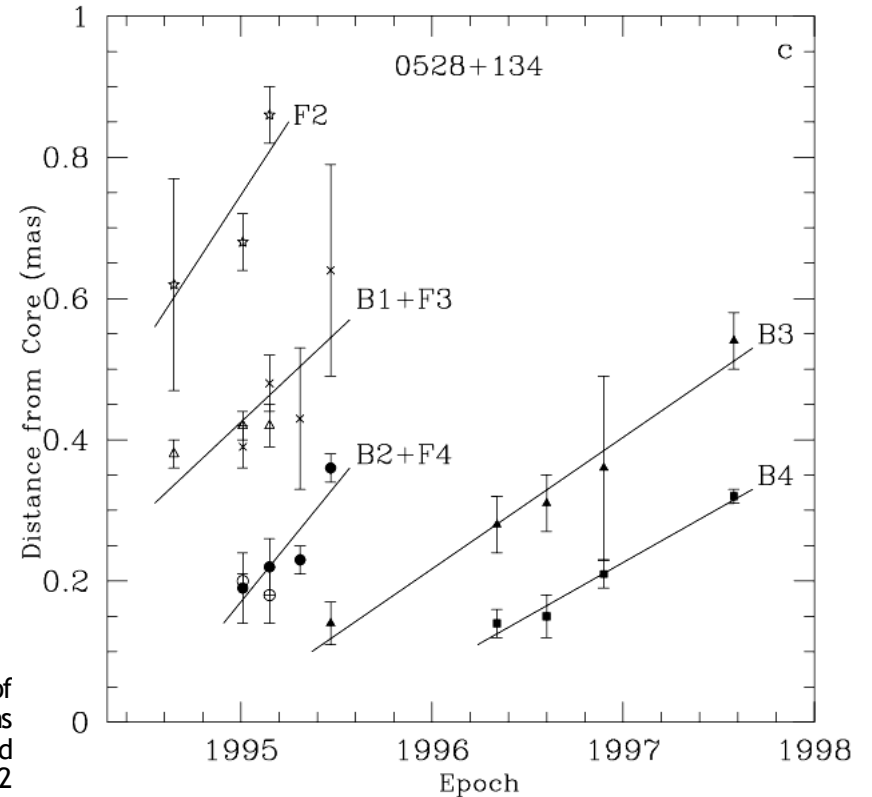


Begelman, Blandford, Rees 1984

# Bulk motion in jets



Jorstad et al. 2001



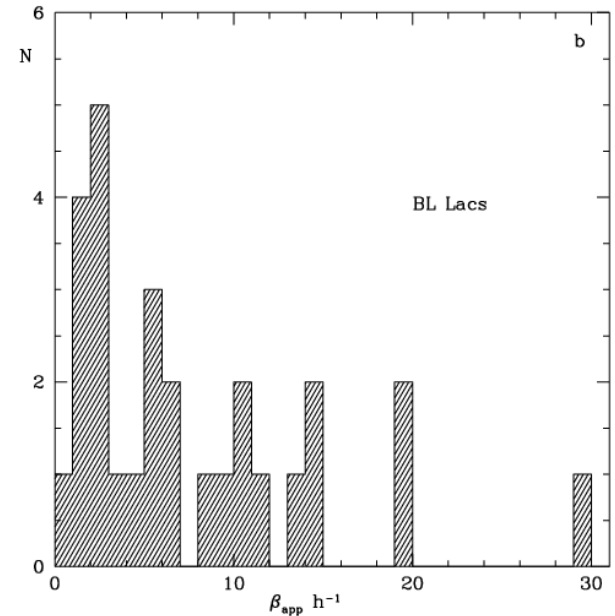
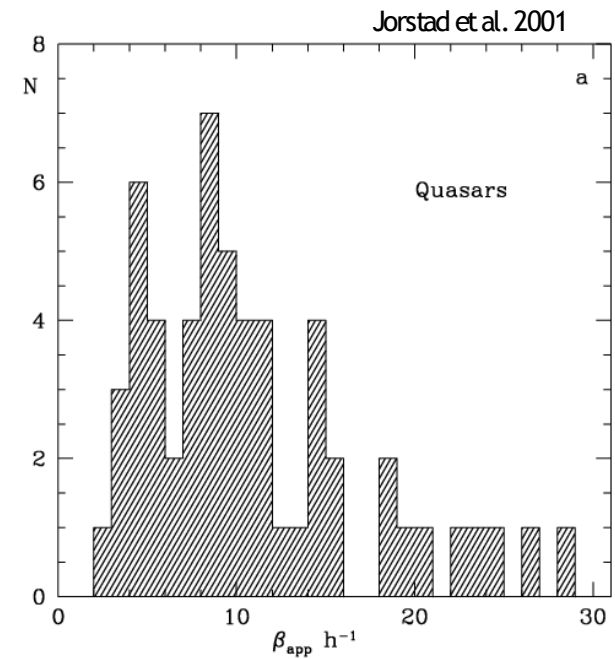
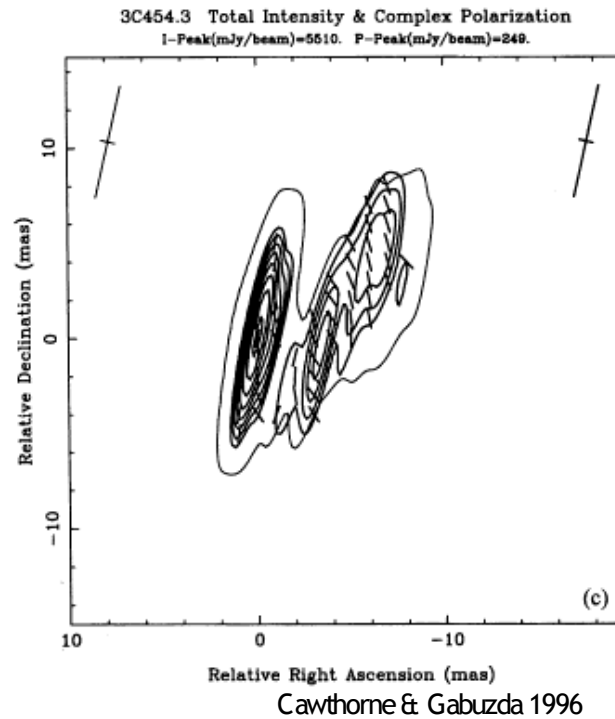
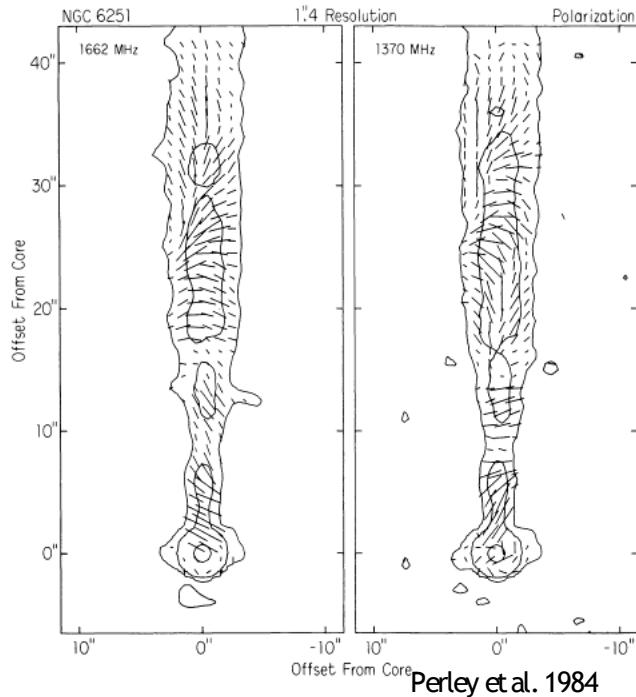
(a) Hybrid maps of 0528+134 at 43 GHz. (b) Hybrid maps of 0528+134 at 22 GHz. (c) Positions of components with respect to the core at different epochs from model fitting for 0528+134; designations of components are as follows. Filled squares: B4 at 43 GHz; filled triangles: B3 at 43 GHz; filled circles: B2 at 43 GHz; open circles: F4 at 22 GHz; crosses: B1 at 43 GHz; open triangles: F3 at 22 GHz; stars: F2 at 22 GHz.

# Bulk motion in jets

- most of the “bright spots” move outward with constant, relativistic speed;
- but stationary spots, accelerating spots, and even inward moving spots are also present
- polarization

## Problems:

- bright spots may not necessary be the indicators of matter flow
- resolution still too low to resolve inner parts of the flow



(a) Distribution of apparent speeds of jet components in quasars. (b) Distribution of apparent speeds of jet components in BL Lac objects.

# Bulk motion in jets

- gamma rays must be relativistically beamed
- in order for gamma rays to escape  $\tau_{yy} < 1$

$$l \stackrel{\text{def}}{=} \frac{L}{r} \frac{\sigma_T}{m_e c^3} \rightarrow l < 40$$

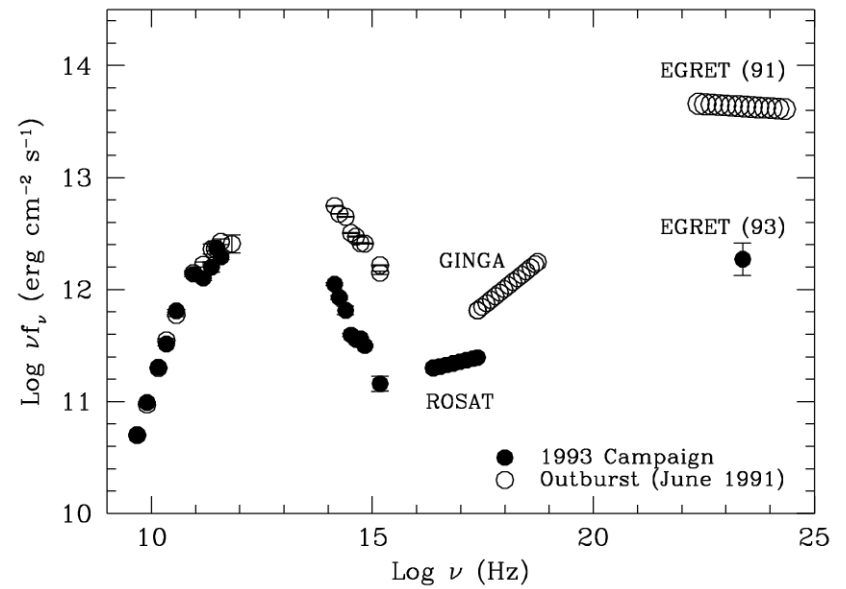
- inferred values for 3C 279 and PKS 0528+134 for the compactness are 5000 to 15,000
- if one assumes relativistic motion

$$L_{obs} = D^4 L \quad r = D c \Delta t_{obs}$$

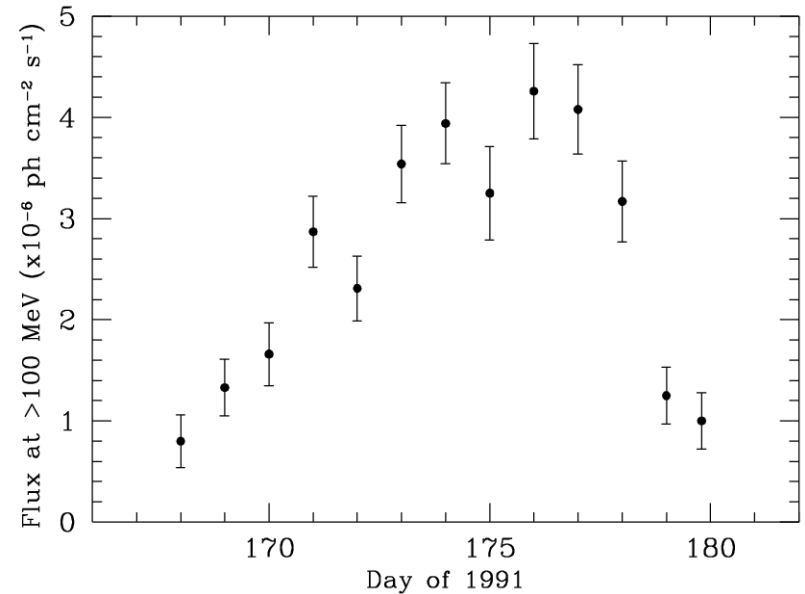
$$l = D^{-5} \frac{L_{obs}}{\Delta t_{obs}} \frac{\sigma_T}{m_e c^4}$$

- condition  $l < 40$  translates into  $D > 6$  for 3C 279 and  $D > 7$  for PKS 0528+134

Urry & Padovani 1995



Multiwavelength spectra of the gamma-ray-bright superluminal quasar 3C279 (Maraschi et al. 1994a) at two epochs, a high state in June 1991 and a low state in January 1993.



Gamma-ray light curve of the superluminal quasar 3C279 during the bright outburst in June 1991 (Kniffen et al. 1993).

# Comptonization close to the black hole

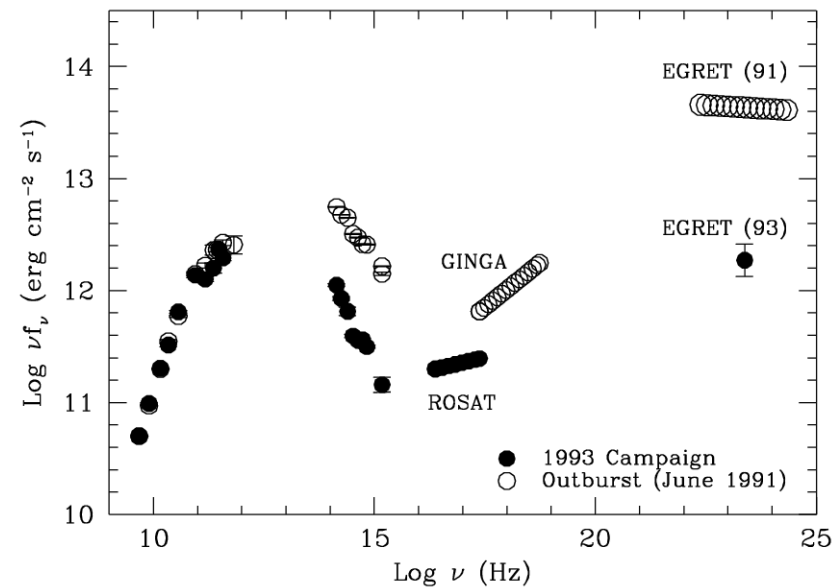
- Begelman & Sikora (1987): "a jet accelerated to relativistic velocities close to the black hole must Comptonize the radiation produced by accretion flow".

## Conclusions:

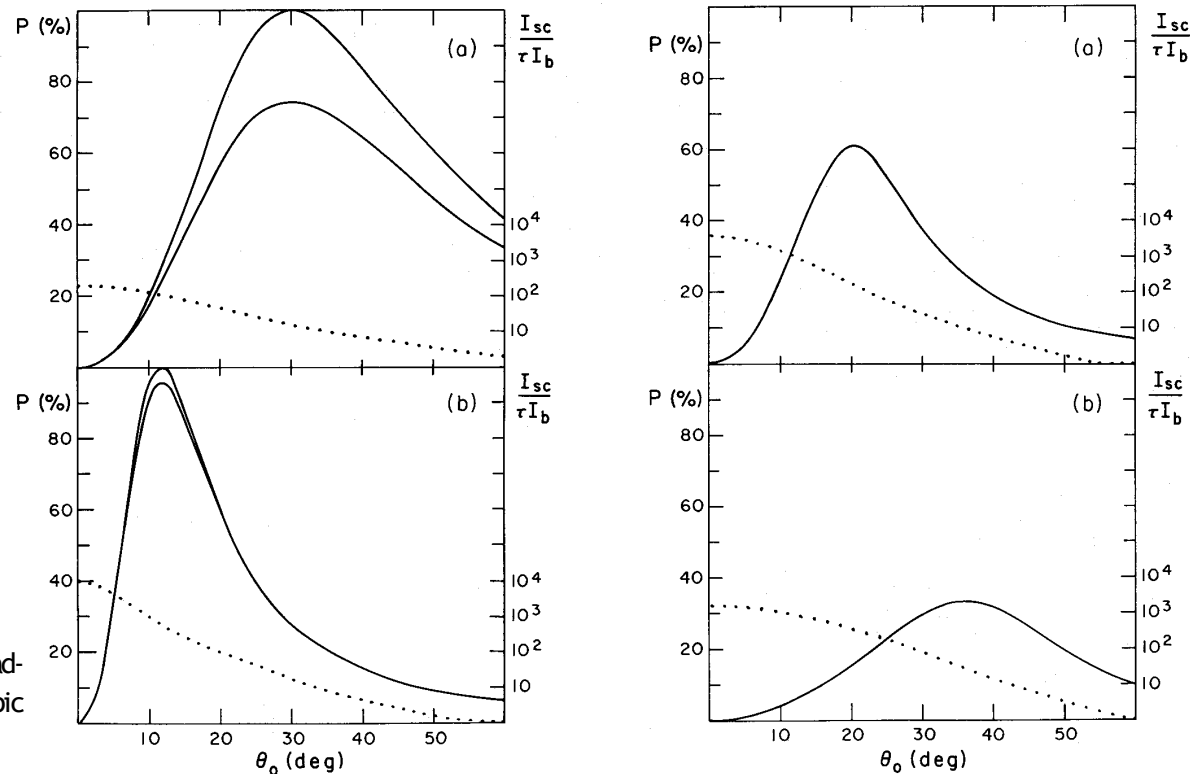
- flux of Comptonized ambient radiation may be responsible for variable IR— X-ray continuum in blazars
- this radiation may be polarized to high degree, with polarization very sensitive to the viewing angle, and electron distribution.

Degree of polarization (P) vs. the viewing angle ( $\theta_0$ ), as computed in the "head-on" approximation (upper solid line) and exactly (lower solid line), for isotropic ambient radiation field with power-law spectrum.

Maraschi et al. 1994



Begelman & Sikora 1987



## Soft X-ray “bump”

- jets are powered at a rate  $10^{46}$ - $10^{48}$  erg/s - such power has to originate deep in potential well (BZ vs. AD) and must be transported to pc scales through dense radiation fields (in case of FSRQ - reprocessed UV radiation)
- cold electrons (in situ acceleration) in a steady jet produce Compton luminosity  $L_{BC} \simeq 2 \Gamma^2 \frac{1}{4} n_e r_{min} \sigma_T \xi L_{UV}$

- which peaks at energy  $h\nu_{BC} \simeq \Gamma^2 h\nu_{UV} \sim \left(\frac{\Gamma}{10}\right)^2$  keV

(typical luminosities  $10^{46}$  erg/s and spectra usually consistent with a simple power law)

- using observational constraint  $L_{BC} < L_{SX}$  it follows that

$$\tau \simeq \frac{n_e r \sigma_T}{\Gamma} < 0.02 \frac{L_{SX,46}}{(\xi L_{UV})_{45}} \left(\frac{\Gamma}{10}\right)^{-3}$$

so **jets must be optically very thin**

- for  $e^+e^-$  jet

$$L_{BC} > 3 \times 10^{47} (\Gamma \theta_j) (\xi L_d)_{45} \left(\frac{\Gamma}{10}\right)^3 \left(\ln \frac{r_1}{r} + 1\right) \text{ erg/s}$$

- if one additionally assumes that  $L_K \sim n'_p m_p c^3 \pi r^2$ , then

$$\frac{r_{min}}{r_g} > 200 \frac{n_e}{n_p} \frac{L_K}{L_{Edd}} \frac{(\xi L_{UV})_{45}}{L_{SX,46}} \left(\frac{\Gamma}{10}\right)^3$$

and **jets must form far from the black hole**

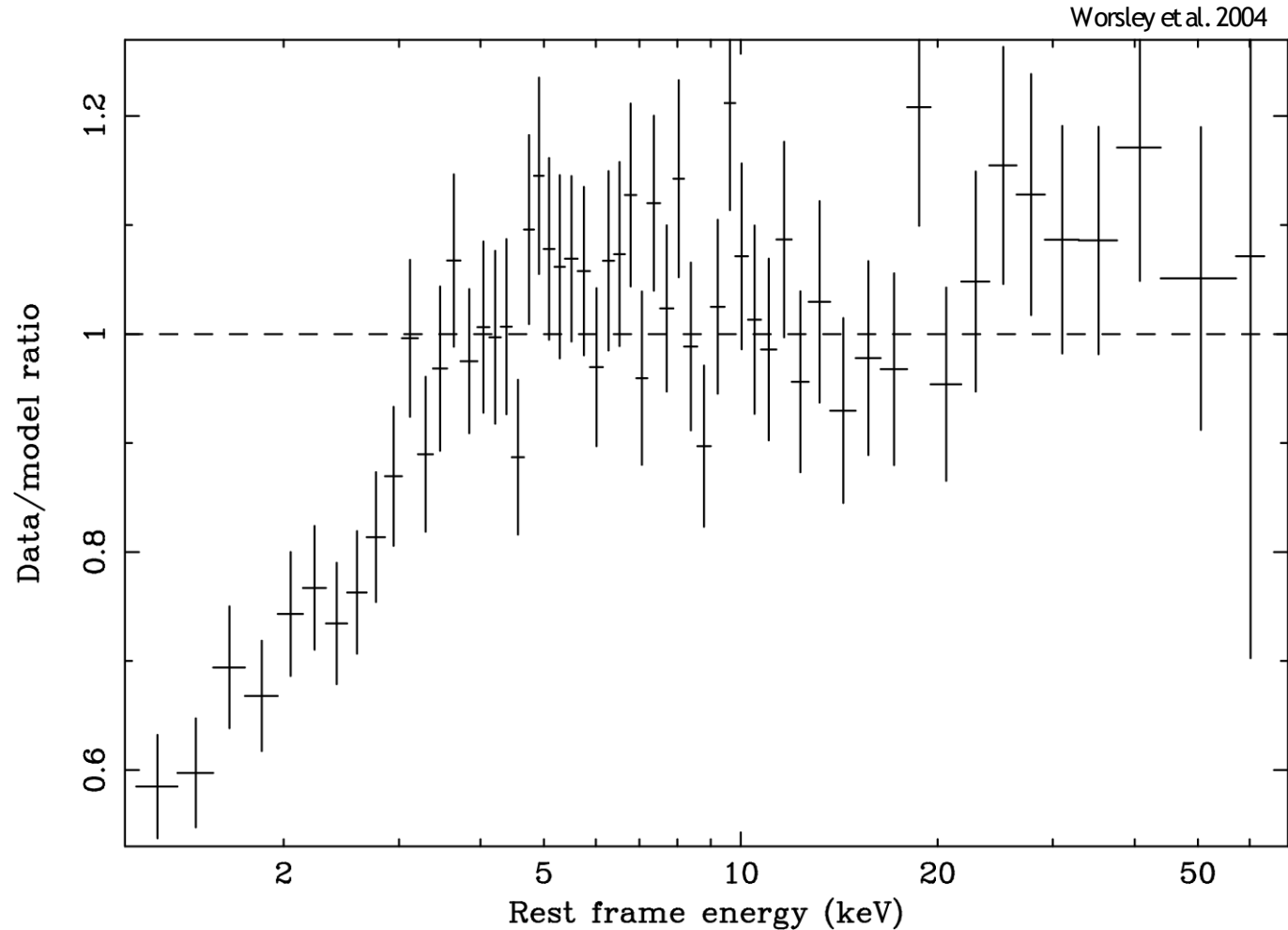
Sikora & Madejski 2000

Celotti & Fabian 1993

## Soft X-ray “bump”

GB B 1428+4217 ( $z=4.72$ )

- studied in the context of additional absorption component in soft X-ray band
- data between 5-12keV (variability and spectral fitting) suggestive of a second inverse Compton component:
  - pile-up in the seed photon distribution
  - different external photon source
  - SSC emission
  - **bulk Compton component**



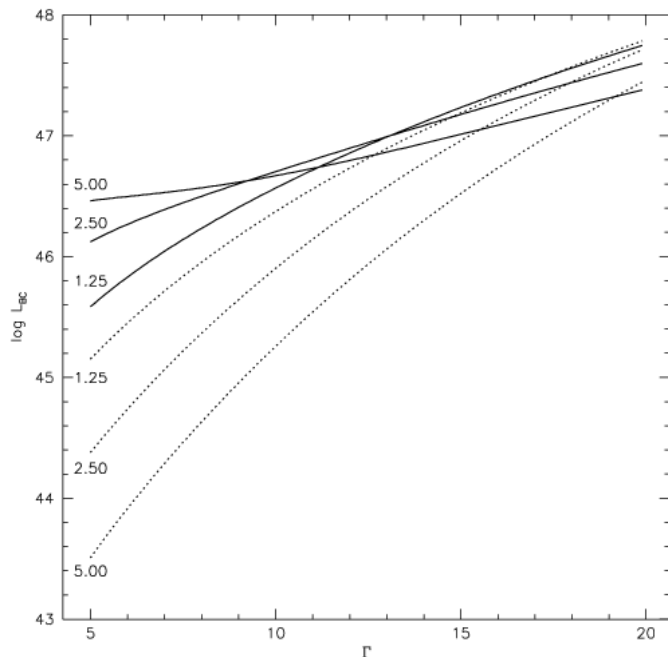
The combined PN camera data of both observations, plotted as a ratio to a fitted  $\Gamma=1.77$  power-law (including Galactic absorption of  $N_{\text{H}} = 1.40 \times 10^{20} \text{ cm}^{-2}$ ). The energy has been adjusted to the source rest frame.

## Soft X-ray “precursors”

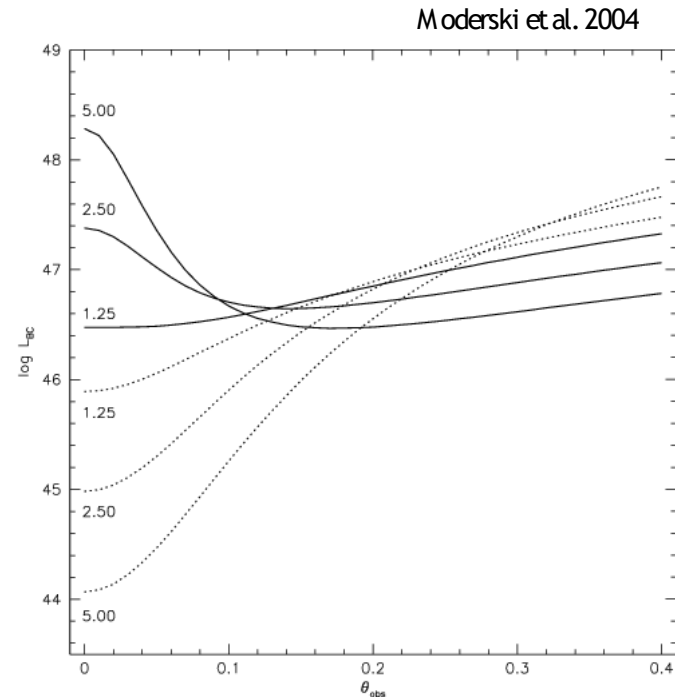
- internal shock model for non-thermal flares in blazars (inhomogeneities moving down the jet with different speeds)

$$\Delta r_{sh} = \beta c t_{fl} D \Gamma \simeq 7.8 \times 10^{17} \left( \frac{t}{3 \text{ d}} \right) \left( \frac{\Gamma}{10} \right)^2 \text{ cm} \quad L_{BC} \simeq D^4 \frac{4}{3} c \sigma_T u_{BEL} \Gamma^2 N_e$$

number of electrons may be inferred from non-thermal flare



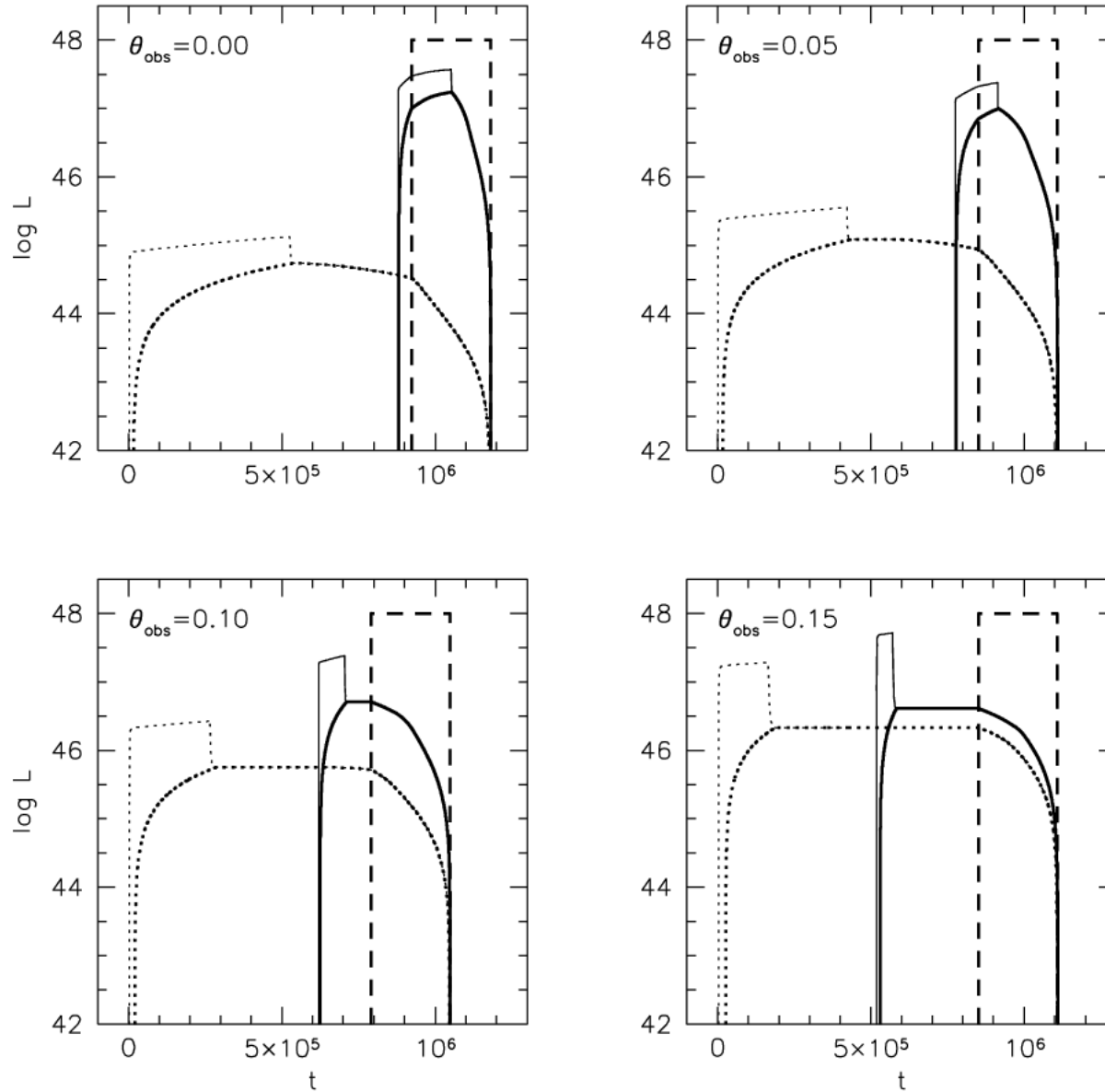
Precursor luminosity as a function of the bulk Lorentz factor . The angle of view is  $\theta_{\text{obs}}=1/10$ , and the three pairs of curves are calculated for ratio of the Lorentz factors of the two shells,  $\alpha=1.25, 2.5$ , and  $5$  (marked beside the curves on the left side of the plot). The solid lines are for the faster of the two shells, and the dotted lines are for the slower of the two shells.



2.— Precursor luminosity as a function of the angle of view  $\theta_{\text{obs}}$ , for  $\Gamma=10$ . Other parameters are the same as in Fig. 1.

# Soft X-ray precursors

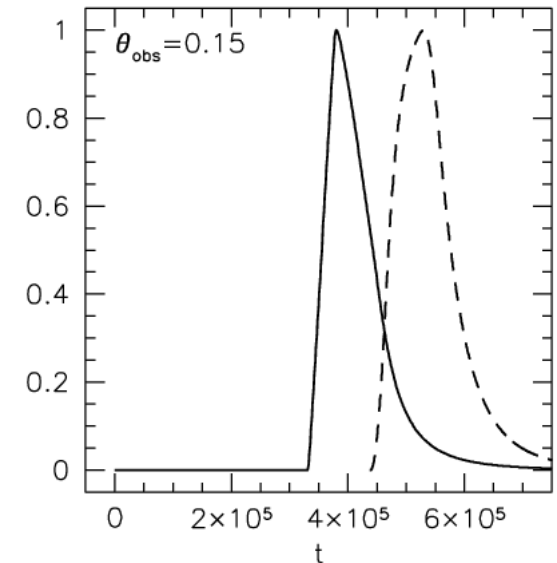
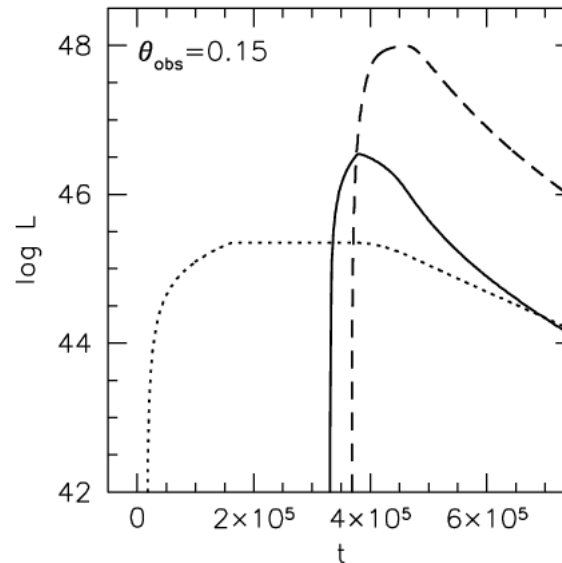
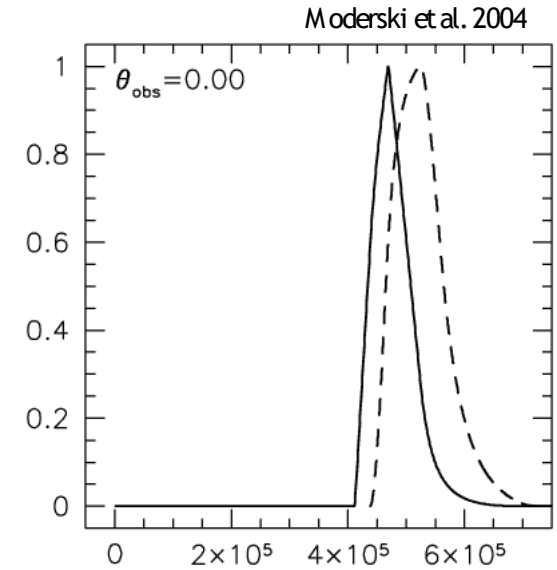
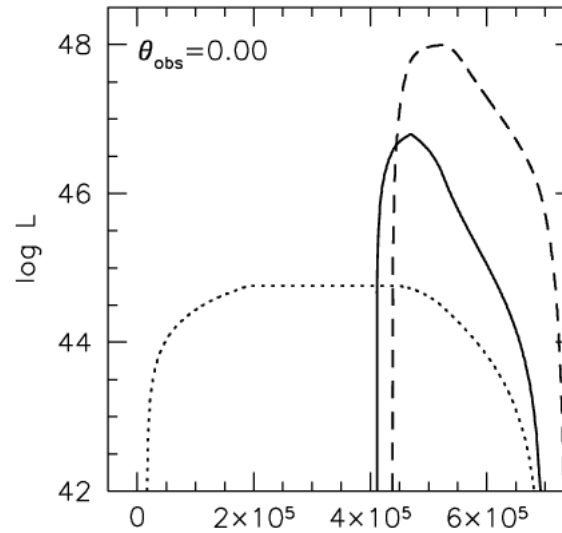
Moderski et al. 2004



Light curves of precursors and flares for four different values of  $\theta_{\text{obs}}$ . The solid lines are for the precursors produced by the faster shells, the dotted lines are for the precursors produced by the slower shells, and the dashed lines are for the nonthermal  $\gamma$ -ray flares as produced deeply in the fast cooling regime.

## Soft X-ray precursors

- precursor from faster shell typically 10-30 times less luminous than non-thermal flares
- should dominate the spectrum in the soft X-ray band even if SSC and EC is included
- precursor from faster shell overlaps with non-thermal flare, but decays faster (easy distinguishable from the flare)

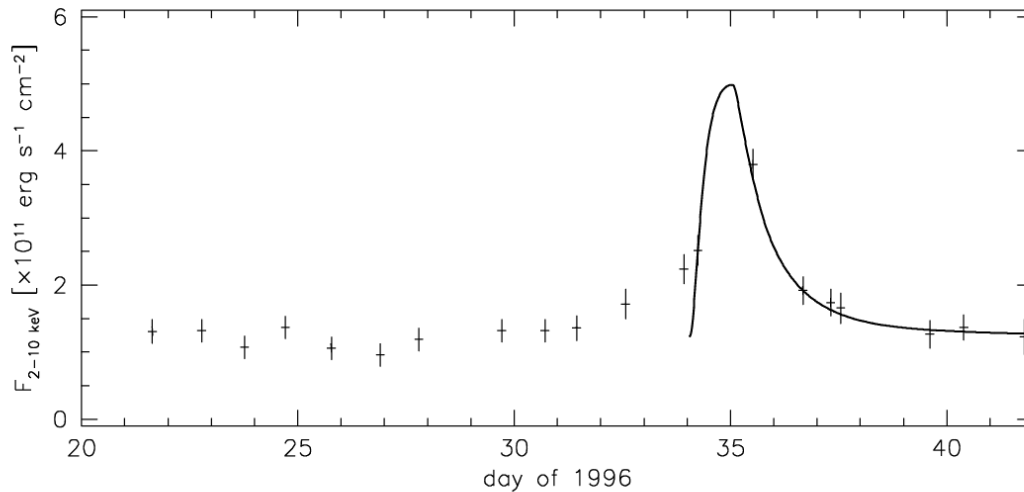
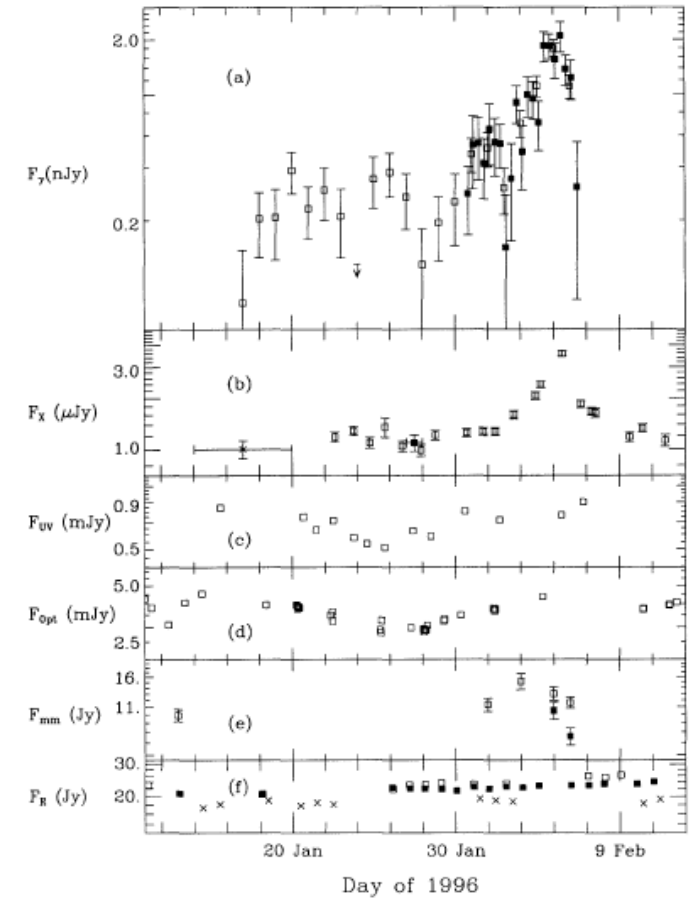
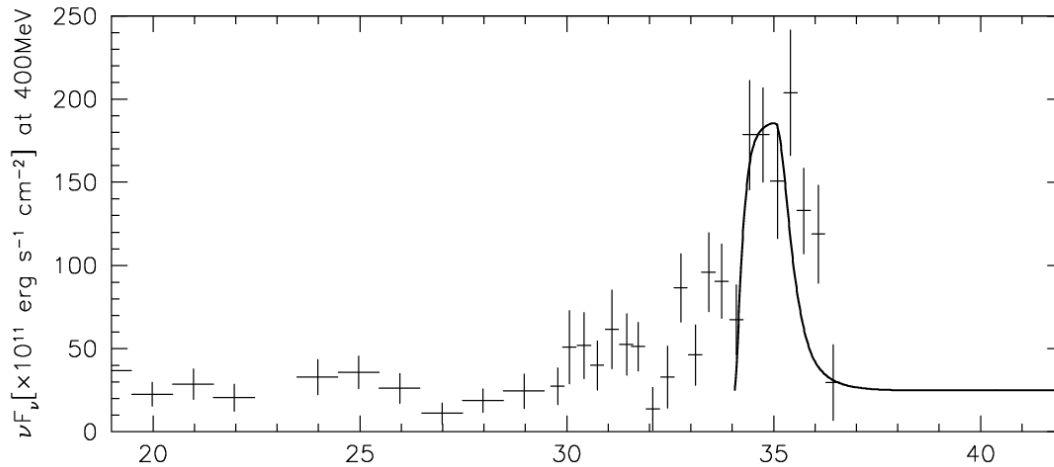


Light curves of the two types of precursors and the nonthermal flares for  $\theta_{\text{obs}}=0$  (top left) and  $\theta_{\text{obs}}=0.15$  (bottom left) for  $\theta_j=1/\Gamma=0.1$ . Those due to the faster shells and the flares are redrawn in linear scale on the right panels with their peaks normalized to one.

# Soft X-ray precursors

Wehrle et al. 1998

Moderski et al. 2003



$\gamma$ -ray (upper panel -  $F_\nu$  flux at 400 MeV) and X-ray (lower panel - integrated 2-10 keV flux) light-curves of the blazar 3C 279 during the Feb '96 flare. Data points are from Wehrle et al. (1998). Thick, solid line shows the light-curves of our model.

- variability (simultaneous observations in X-rays and gamma with intra-day resolution: GLAST+X)
- polarization (different for BC and SSC)
- flux of particles vs. Poynting flux
- *in situ* inhomogeneities formation vs. direct acceleration in reconnection sites

## Bulk Comptonization at larger scales

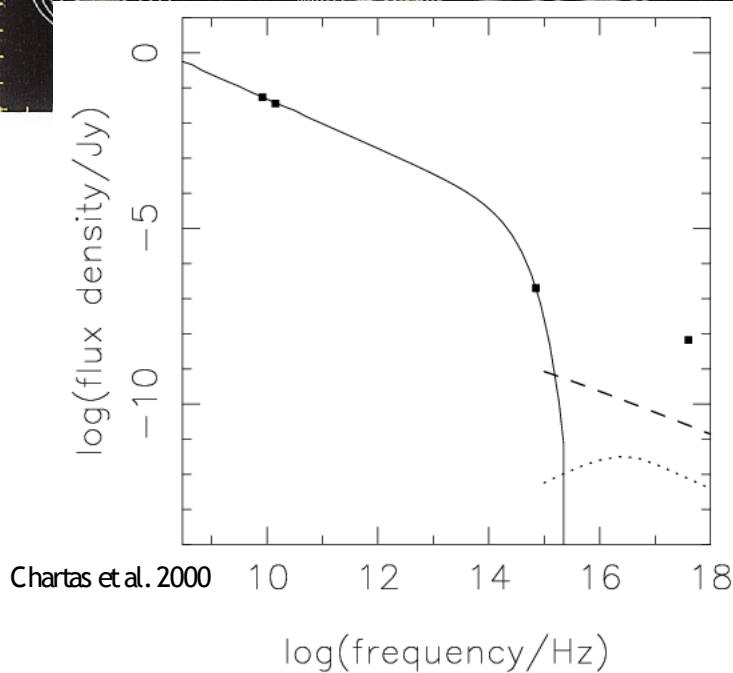
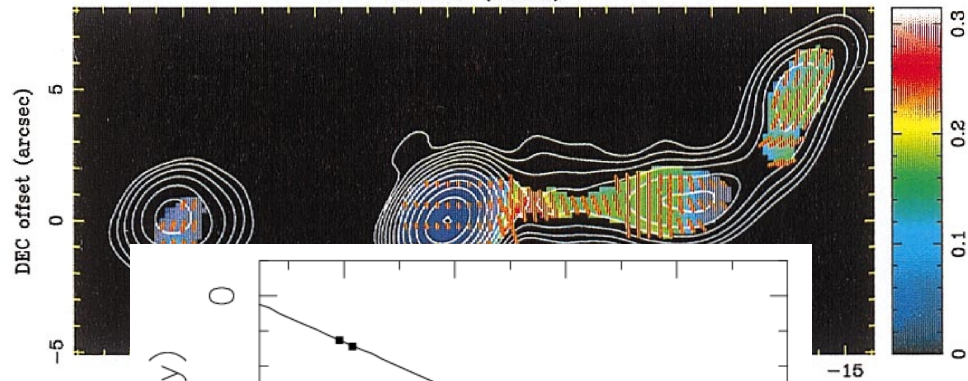
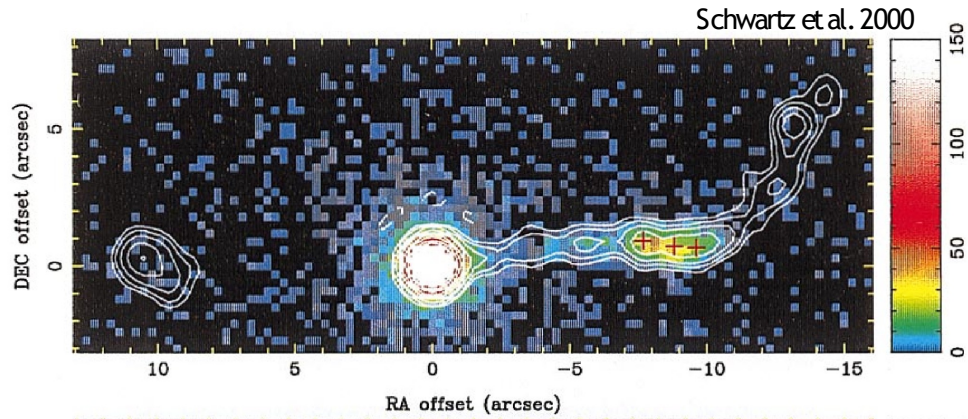
### Problems:

- no direct observations of inner region: unknown distance of jet formation, density and size of broad line region (e.g. variable  $\xi$ ), geometry of the jet (opening angle)
- precursor or bump may be hidden in non-thermal continuum

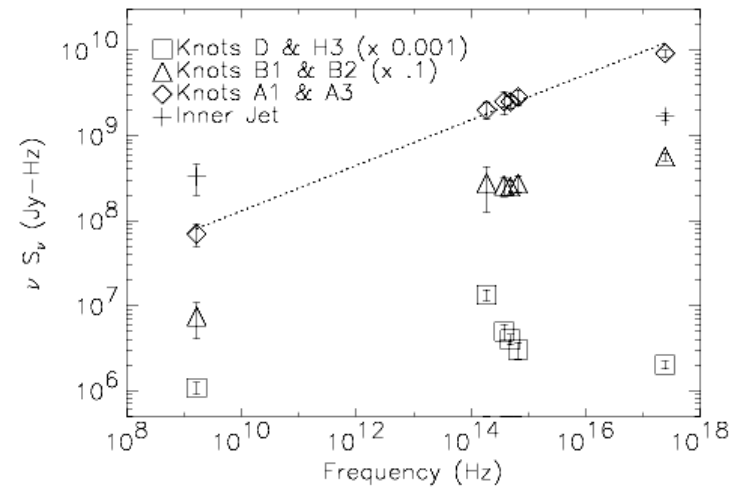
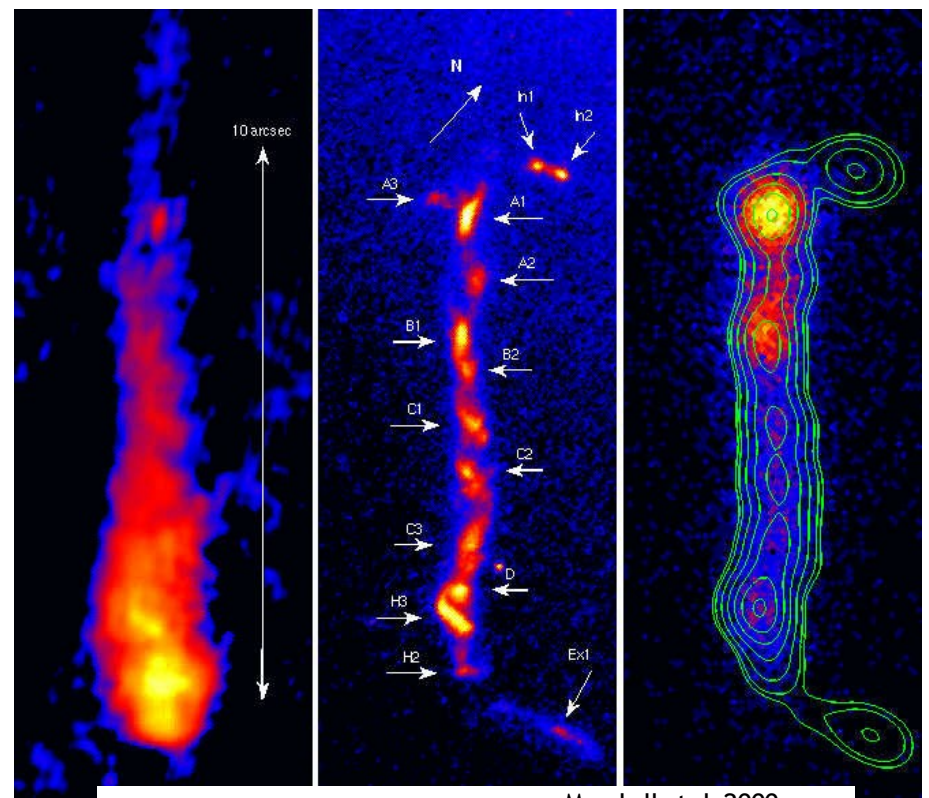
### Solution:

- look for better objects with known geometry of the flow and target photon distribution

# Bulk Comptonization at larger scales



Spectral energy distribution for knot WK7.8 in the PKS0637-752 jet. The solid line is the synchrotron component, the dashed line is the SSC component, and the dotted line is the Compton-scattered CMB component.



Spectral energy distributions (SEDs) of the 3C 273 jet knots A1, B1/B2, D/H3, and the inner jet. The overall spectrum of knot A1 fits a simple power law, shown as the dashed line with a slope of 0.25, so the spectrum is consistent with a simple synchrotron model with a single power law distribution of electrons. For knot B1, however, the SED appears to flatten between the radio and optical bands. A single synchrotron model does not fit the SED of the D/H3 region.

## Bulk Comptonization at larger scales

- negligible Compton drag

$$\frac{\Delta \Gamma}{\Gamma} \simeq 1.4 \times 10^{-6} \Gamma_{10} l_{100 \text{ kpc}} (1+z)^4$$

- luminosity

$$L_{BC} \simeq 1.4 \times 10^{-4} l_{100 \text{ kpc}} \Gamma_{10}^3 (1+z)^4 L_e$$

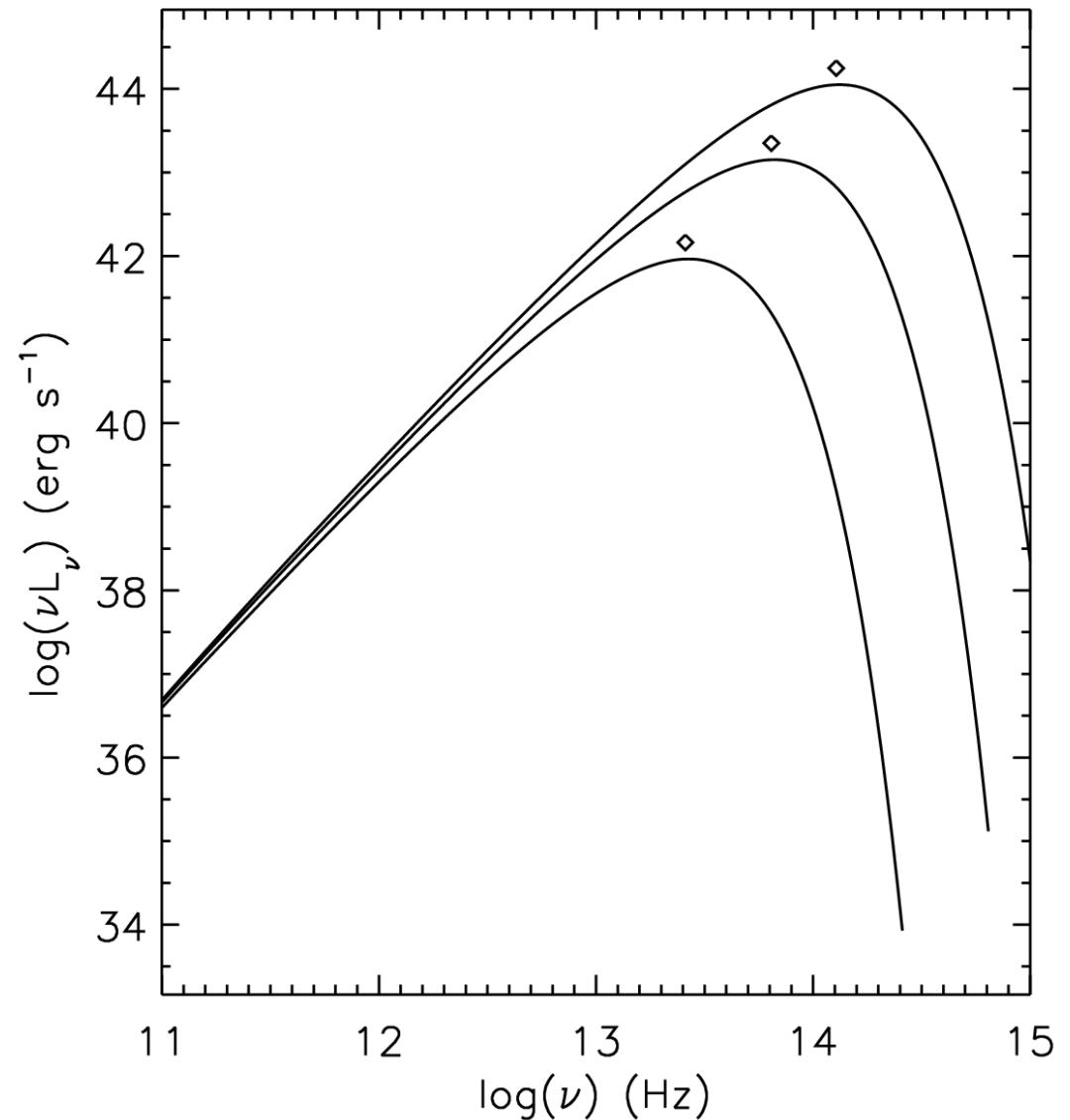
- peaks in the IR regime

$$\nu_{BC} \simeq 4 \times 10^{13} \Gamma_{10}^2 \text{ Hz}$$

- BC surface brightness is independent of  $z$  (cosmological decrease by  $(1+z)^4$  compensated by the increase in of the CMB energy density

- peak frequency is also independent of  $z$   
 - possibility to detect "silent" jets to any redshift

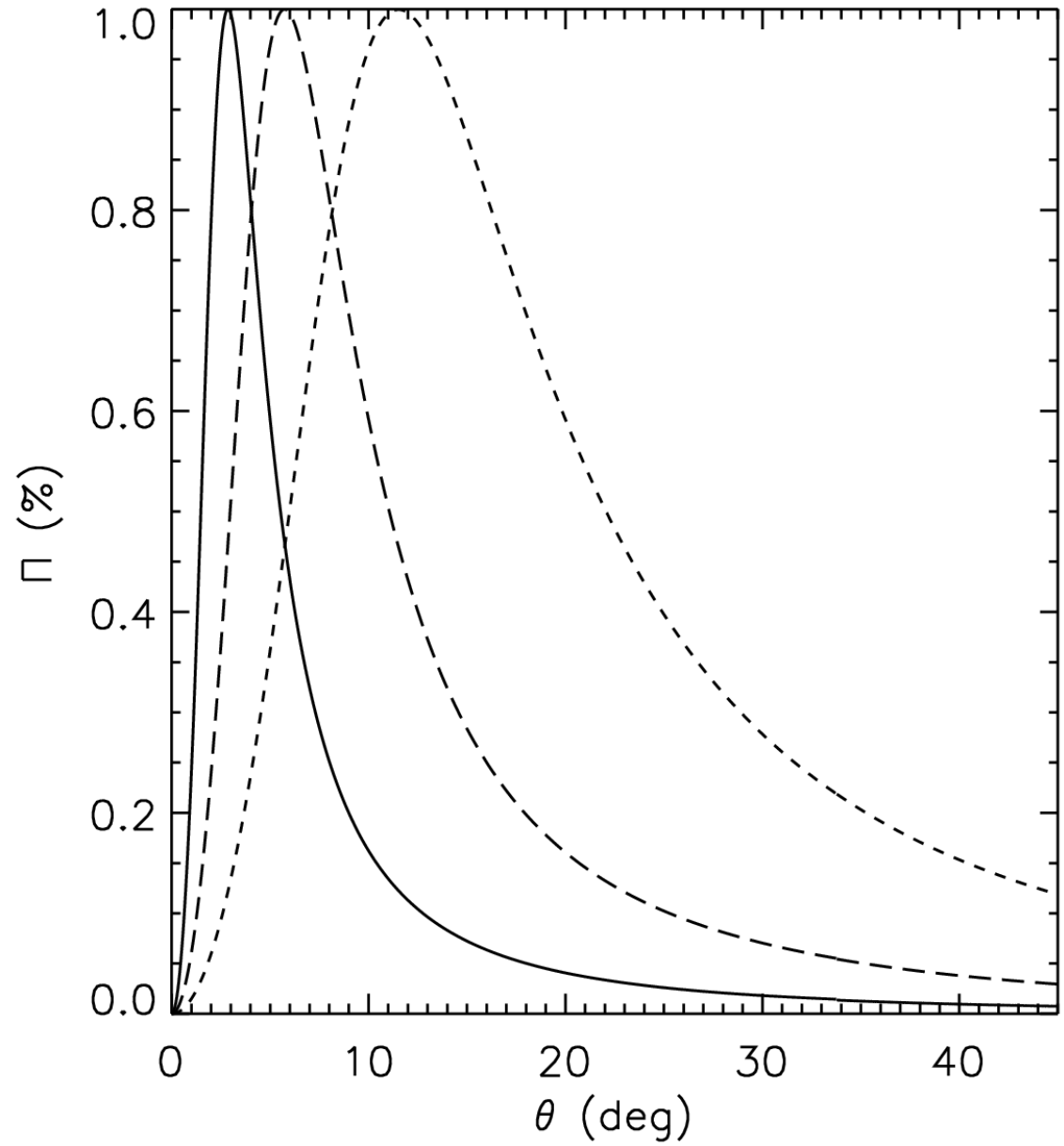
Georganopoulos et al. 2005



Bulk Compton luminosity of a cold electron beam of power  $L_e = 10^{46}$  ergs  $s^{-1}$  propagating with a bulk Lorentz factor  $\Gamma = 10$  for a distance of 100 kpc through the CMB at  $z = 1$ .

## Bulk Comptonization at larger scales

Georganopoulos et al. 2005



- polarization measurements together with peak frequency may provide independent estimations of both the bulk Lorentz factor and the angle of view

Bulk Compton emission polarization from a cold electron beam as a function of observing angle for  $\Gamma=20$  (solid curve),  $\Gamma=10$  (long-dashed curve), and  $\Gamma=5$  (short-dashed curve).

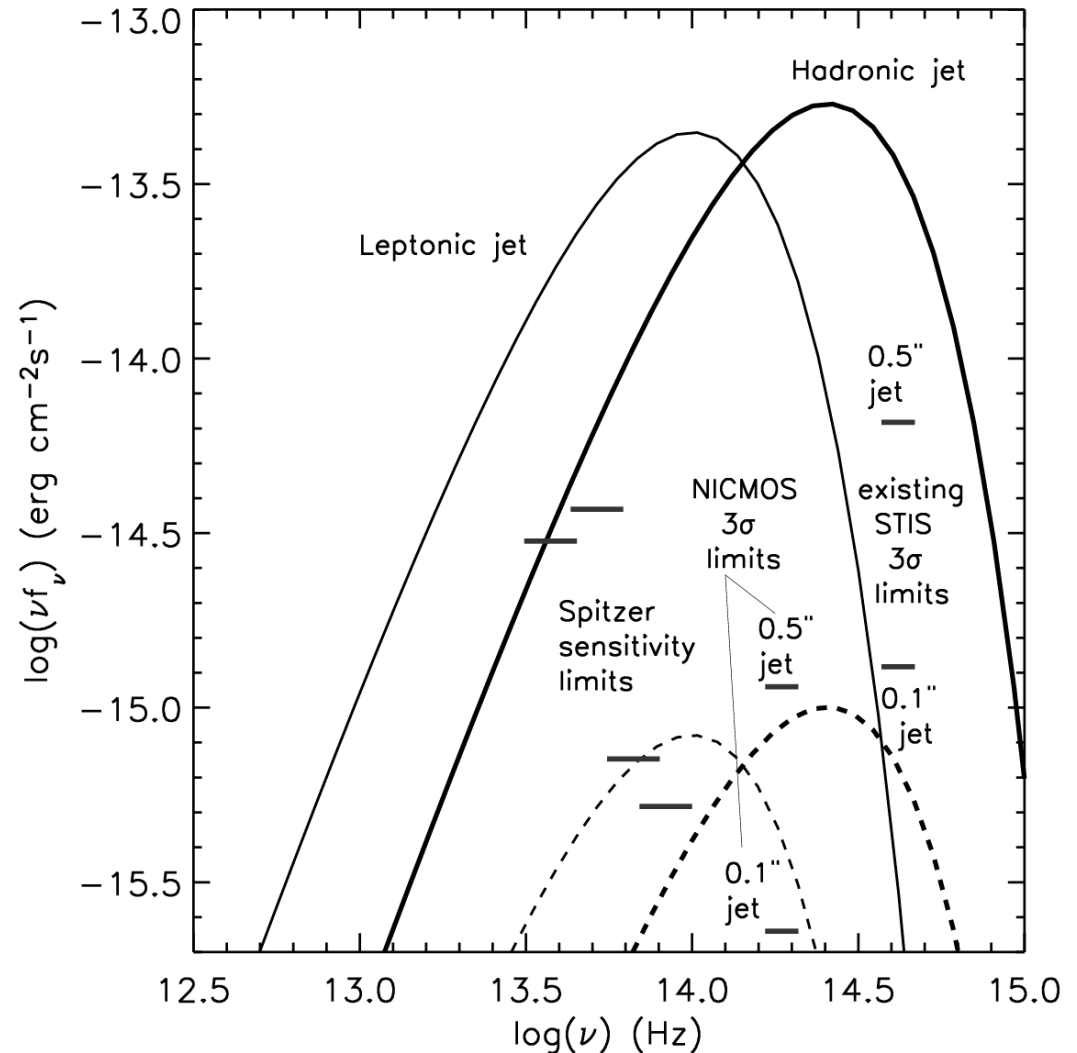
## Bulk Comptonization at larger scales

### PKS 0637-752

- two cases: case A (all required lepton power in the knot is provided by cold lepton in a jet - most optimistic) and case B (jet provides only number of leptons - most conservative); both in two flavours: "leptonic" and "hadronic".

- minimum power Doppler factor (Dermer & Atoyan 2004):  $D_{\min} = 17.4$  (27.8); minimum jet power  $L_{\min} = 9.7 \times 10^{45}$  ( $6.3 \times 10^{46}$ ) [erg/s]; jet length  $l = 930$  (1500) [kpc]

Georganopoulos et al. 2005

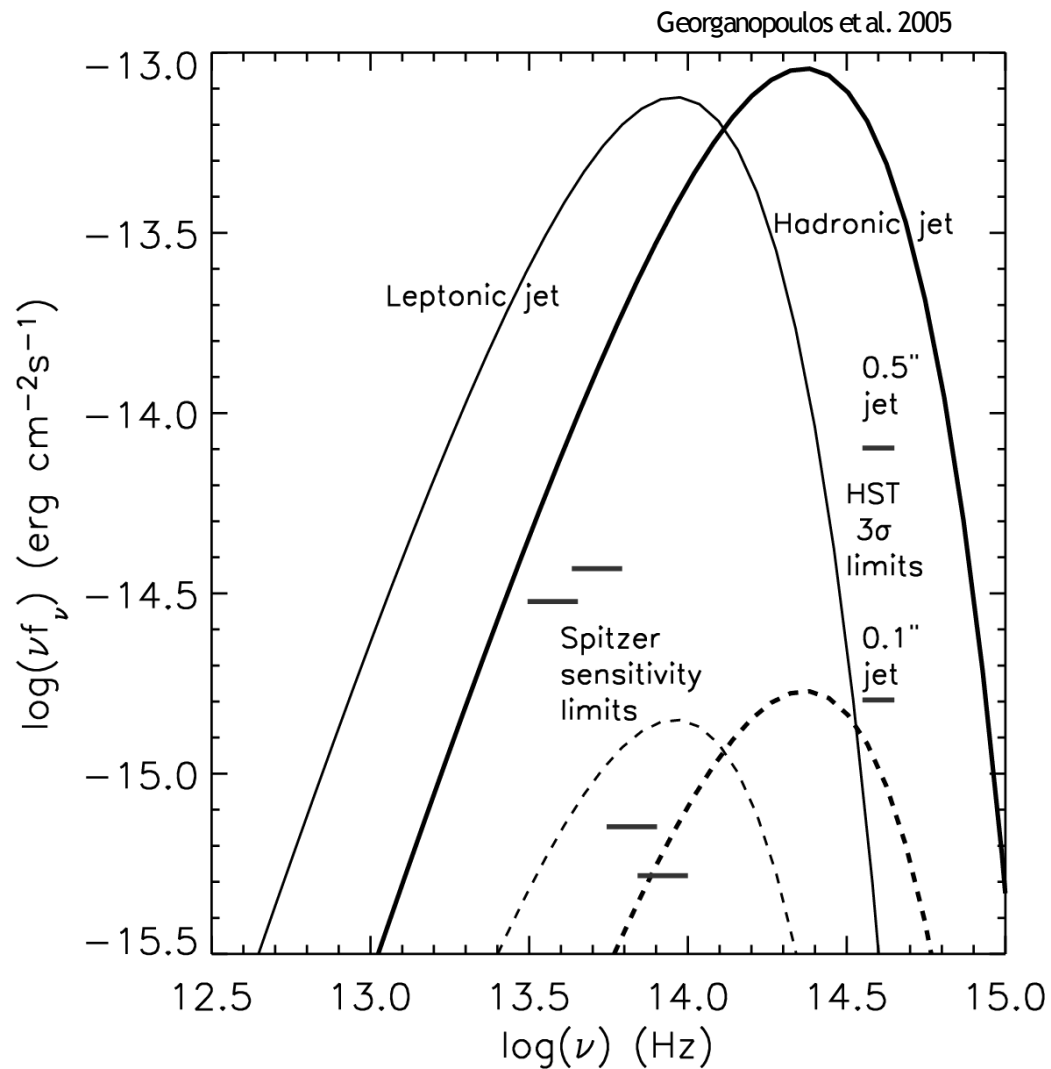


BC emission for a leptonic (thin solid curve) and a hadronic (thick solid curve) jet composition of PKS 0637752 for case A, in which the lepton power  $L_{\text{lept}}$  required in the knot is provided by the cold leptons in the beam. The dashed curves correspond to case B, in which the jet provides simply the number of leptons needed in the knot, with the thin and thick curves representing a leptonic and a hadronic jet composition, respectively. The Spitzer sensitivity limits, existing  $3\sigma$  HST STIS limits (see text), and expected  $3\sigma$  HST NICMOS  $\lambda = 1.6 \mu\text{m}$  limits for a three-orbit exposure, assuming a  $0''.1$  or a  $0''.5$  jet radius, are also shown.

## Bulk Comptonization at larger scales

### 3C 273

- minimum power Doppler factor:  $D_{\min} = 16.6$   
(26.5); minimum jet power  $L_{\min} = 3.3 \times 10^{45}$   
( $2.1 \times 10^{46}$ ) [erg/s]; jet length  $l = 930$  (1500) [kpc]



Same as in previous, but for 3C 273. HST ACS limits are derived from Martel et al. (2003).

## Conclusions

- the process of **bulk Compton** scattering is important, as long as there are **cold electrons** propagating in a jet
- the process operates from **sub-parsec** to **kilo-parsec** scales
- the process provides constraints on **jet composition**, **distance of jet formation**, **magnetic field role**, **orientation** of the jet and its **bulk Lorentz factor**
- there is a growing **observational evidence** that the **bulk Compton** process operates in blazars and in kilo-parsec scale jets of superluminal quasars
- near future: *Spitzer* observations of kpc jets (poster 49 by Y. Uchiyama) and **simultaneous GLAST X-ray** observations of non-thermal flares in blazars
- future: **X-ray polarimetry** (but questionable if electrons are not really cold)